Numerical Simulation of In-Plane Damage Progression in Laminated Composite Plates

Kevin V. Williams[1], Anthony M. Floyd[2], Reza Vaziri[2], and Anoush Poursartip[2]

[1]*Numerical Simulations Group (Materials), Weapons Effects Section, Defence Research Establishment Valcartier, 2459 Pie-XI Blvd. North, Val-Bélair, Québec, G3J 1X5, Canada*

[2]*Composites Group, Departments of Metals & Materials Engineering and Civil Engineering, The University of British Columbia, 309-6350 Stores Road, Vancouver, British Columbia, V6T 1Z4, Canada*

SUMMARY: A new continuum damage mechanics (CDM) constitutive model, UBC-CODAM3Ds, is developed and implemented in the commercial finite element hydrocode LS-DYNA3D. The motivation for model development is to simulate damage progression, and therefore energy absorption, in composite materials subjected to a variety of loading conditions. In this paper, results of the application of the model to the prediction of the force-displacement response and damage growth in a quasi-statically loaded **O**versized **C**ompact **T**ension (OCT) specimen are presented. The predictive capability of the model is demonstrated through successful comparisons between the measured and predicted load-displacement response as well as the overall damage zone size.

KEYWORDS: Strain softening, damage growth, continuum damage mechanics, constitutive model, energy absorption

INTRODUCTION

Rapid growth in the use of composite materials in structural applications has created the need for a detailed understanding of damage tolerant and damage resistant design. Given the complexity and multitude of damage mechanisms that can occur in composite materials, their overall mechanical behaviour is highly nonlinear and extremely difficult to model. From a practical point of view the only viable approach to modelling the nonlinear response of composite structures is to quantify damage development on a macroscopic basis. This entails construction of continuum models that permit accurate quantification of the damage progression and the resulting loss of stiffness.

Recent research [1,2] indicates that damage growth in a polymeric composite structure manifests itself in the form of overall strain softening of the material. Strain-softening models have received a great deal of attention for describing the fracture of concrete and other heterogeneous brittle materials. In general, a macroscopic description of damage can be captured by a constitutive model that exhibits a decrease of stress with increasing strain beyond some critical strain. Computationally, this goal can be achieved through continuum

damage mechanics (CDM) theories [3,4] in which the net effect of fracture is idealized as a degradation of the elastic modulus of the material. The required homogenization techniques and the resulting smearing of material properties play a critical role in the response predictions. Therefore, a close link between experimental and modelling work is essential for the success of this approach.

MODEL FORMULATION

A physically realistic CDM-based model for laminated composite materials has been developed and implemented [5,6] into the nonlinear, explicit finite element code, LS-DYNA3D [7]. In recognition of the fact that the laminate response is driven not only by the lamina properties but also by the ply interactions through the stacking sequence and damage growth [8], the formulation is focussed on the behaviour of a sublaminate as the basic building block. A sublaminate is typically a repeating unit of laminae in a laminate stack (e.g. [0/45/90/-45] in a $[0/45/90/-45]_{3S}$ laminate).

All CDM models provide a mathematical description for the dependence of the elastic coefficients on the damage state and the evolution of damage with the loading state. However, one of the most difficult tasks associated with applying many of the available CDM models has been the measurement of the material parameters required for their characterization. Typically, CDM models have used a simple predefined stiffness reduction function, for example a linear relation, in conjunction with a more complex damage growth law such as a Weibull function. The damage laws are frequently complex and the means of determining the required parameters are often not clear.

In the composite damage model developed at UBC (CODAM3Ds), both the damage growth function and the modulus reduction functions have been carefully chosen to be representative of currently available and published experimental observations (e.g. [9,10]). Where there is a lack of experimental data, simple analytical tools, such as classical laminate plate theory, and the ply-discount method, are used to estimate the required constants.

The CODAM3Ds model is based on three behaviour regimes in the material response: *undamaged elastic*, *damage phase 1* (matrix dominated), and *damage phase 2* (fibre and matrix dominated). Each is characterized by a different relationship between the damage variables and the loading state. The simplest and most flexible approach to capture the changes in damage growth is to assume a linear relationship within each of these regions resulting in a bilinear damage growth curve. An example of this curve for a quasi-isotropic [-45/90/45/0] T300H/F593 CFRP sublaminate is shown in Fig. 1a, where the damage (characterized by the fraction of the total area that is damaged) is plotted as a function of the damage growth potential (characterized by the applied strain). The simulations discussed in this paper are based on specimens made from T300H/F593.

It is assumed that initial damage in the form of matrix cracking commences in the brittle F593 matrix at ≈0% strain, while complete rupture of the laminate occurs at 3.2% strain. This latter value is obtained from quasi-static tests on ligaments of material taken from the process zone in notched **O**versized **C**ompact **T**ension (OCT) specimens [2]. The rate of matrix damage growth (the dashed line in Fig. 1a) is determined by the portion of the damage attributed to matrix cracking at rupture, which depends on the lay-up of the laminate. For the sublaminate considered here, matrix cracking in all 3 off-axis plies (45, 90 and -45) would amount to approximately 80% of the total damage. Following the same argument for fibre breakage, a threshold strain for the onset of fibre damage (for carbon fibres this is roughly between

1.2-1.4% strain) and the proportion of the total damage that can be attributed to fibre failure can be defined. Since the saturation of matrix cracking in this case corresponds to 80% damage, the maximum percentage of total damage attributable to fibres is 20%.

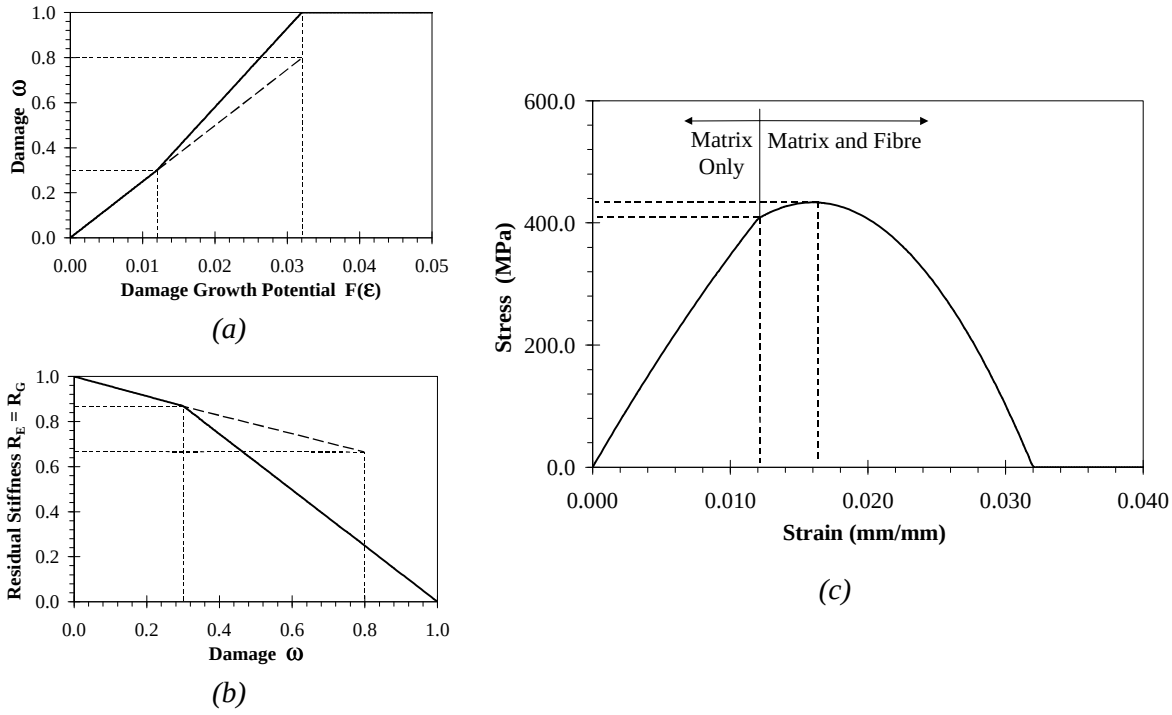

Fig. 1: Strain softening stress-strain curve for T300/593 [-45/90/45/0] CFRP based on bilinear damage growth and residual stiffness functions.

The amount of damage sustained by the sublaminate will affect each of the material moduli to varying degrees. Clearly, the modulus reduction is a function of both matrix and fibre damage and one would expect the rate of stiffness loss associated with each damage mode to be different. Therefore, the modulus reduction is also assumed to be a bilinear function of the damage parameter as shown in Fig. 1b. In constructing this curve it is assumed that at saturation of matrix cracking the off-axis plies do not contribute to the stiffness of the sublaminate, which leads to a complete decoupling of the plies. Using the ply-discount method, the residual stiffness in this case will be approximately 65% of the original undamaged value. Fibre breakage is considered to be the major driver of the stiffness loss with the sublaminate losing its entire stiffness at rupture. The net result of using bilinear curves to represent both the damage growth and stiffness reduction curves is a strain-softening type stress-strain curve as shown in Fig. 1c.

NUMERICAL SIMULATIONS

Kongshavn and Poursartip [2] carried out an experimental investigation with the goal of characterizing damage growth in notched composite laminates. Results included force-displacement curves, displacement field analyses, and damage growth characterizations for an OCT specimen, which was specially designed to achieve stable growth of damage. The geometry of the OCT specimen is shown in Fig. 2. The specimen was loaded quasi-statically in an Instron testing machine. Lateral support for the specimen was provided by two Teflon coated steel bars loosely clamped on either side of the specimen at the edge opposite to the notch. These supports were intended to inhibit through-thickness deformation and warping of the specimen under load.

A number of measurement techniques were employed during the test series in order to characterize the growth of damage in the notched specimens. First, the force-displacement curve was measured by recording the applied load and the displacements at the pinhole (hereafter referred to as the cross-head displacement) and ahead of the notch tip using a clip gauge (see Fig. 2). A unique feature of these tests was the measurement of the displacement field on either side of the crack and growing zone of damage. A series of lines were inscribed on some of the specimens (highlighted in Fig. 2). Through digital photographic analysis, Kongshavn and Poursartip were able to measure changes in the displacement field caused by damage growth. Post-test non-destructive and destructive characterizations of damage included pulse-echo ultrasonic (PEUS) scans, deplies, and micrographical cross-sectional analyses.

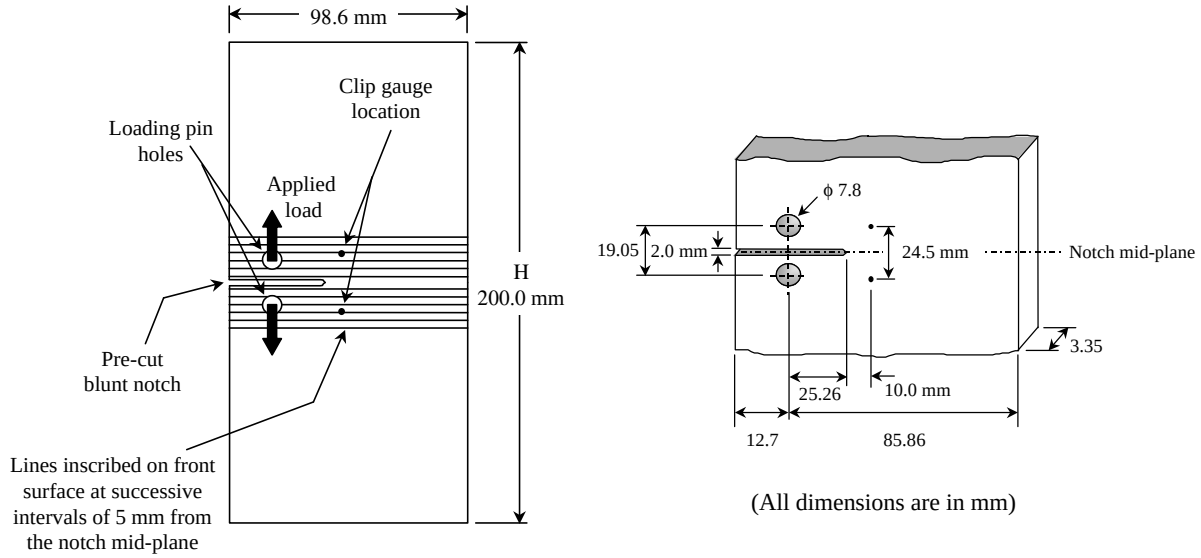

Fig. 2: Overheight compact tension (OCT) specimen geometry. (Adapted from Ref. 2)

Of the specimen geometry and material combinations investigated by Kongshavn and Poursartip, a T300H/F593 $[-45/90/45/0]_{2S}$ quasi-isotropic CFRP panel ($\rho = 1543$ kg/m^3, $E_x = E_y = 38.98$ GPa, $G_{xy} = 14.85$ GPa, $\nu_{xy} = 0.313$, $t_{sublam} = 0.809$ mm) with an a/W ratio (i.e. notch length-to-specimen width ratio) of 0.29 was used as the basis for the modelling work presented here. The elastic constants quoted above were derived from the available lamina values [11] using classical laminated plate theory. The characterization of the damage growth and stiffness reduction functions for this material has already been presented as the example in the Model Formulation section above.

The OCT specimen investigated by Kongshavn and Poursartip offers a good test case of the CODAM3Ds model as the impetus for the experimental study was the characterization of the strain softening behaviour in laminated composites. This behaviour forms the basis for the theoretical development of the model. In effect, by modelling these tests we come full circle with the experimental evidence for progressive damage growth in laminated composites. This is not the first attempt at modelling the OCT test results. Work published by Williams et al. [12] outlines a similar numerical study based on the implicit finite element code, ABAQUS. The results of their work demonstrated the need to incorporate a strain softening material model in order to obtain the overall material response observed experimentally. However, the material model used in the study was an adaptation of a simple orthotropic plasticity model with plastic softening instead of plastic hardening. The study described here represents a significant advance over the ABAQUS model.

Finite Element Model

The finite element model of the OCT specimen is shown in Fig. 3. The deformable specimen was modelled using the four-noded, Belytschko-Tsai plane-stress shell elements. A segment of the loading pin was also modelled using the same plane-stress elements. Only half of the OCT specimen was modelled with symmetry enforced by appropriate translational and rotational displacement boundary conditions placed along the notch mid-plane starting at the location of the notch tip. An additional out-of-plane translational constraint was applied to all nodes in the model to mimic the experimental constraint on through-thickness bending and twisting. The shape of the mesh was constrained by the requirement that elements in the damage growth zone must be of uniform size and shape (i.e. square). Outside of this zone, the mesh size sensitivity of the damage model is not an issue and it is possible to use mesh grading to optimize the mesh.

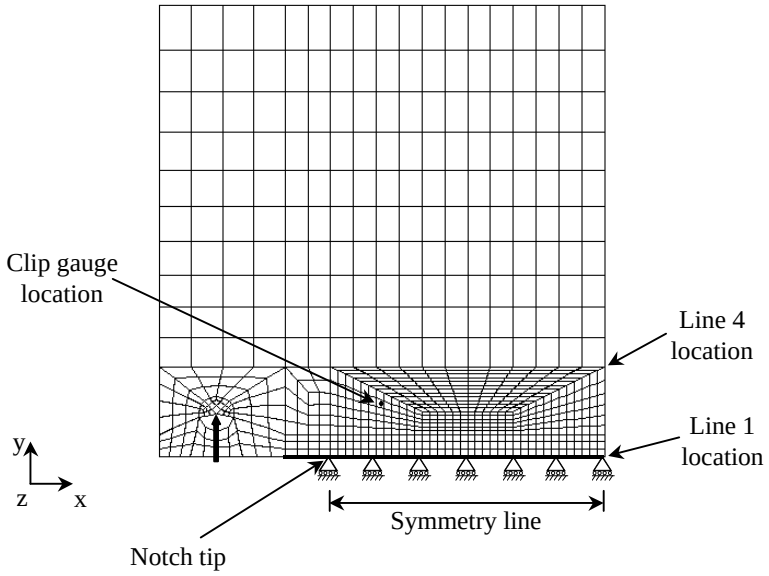

Fig. 3: Schematic of the OCT finite element model.

Note that the local notch tip geometry was not modelled explicitly. Results of the work by Williams et al. [12] showed that the omission of a detailed description of the notch tip did not affect the overall results of the numerical work carried out as part of that investigation. In the experiments, the notch was blunt so as to give a less localized stress distribution, and thus a large damage zone.

Loading of the specimen was achieved by applying a monotonically increasing y-displacement to the loading pin. A number of preliminary runs were performed to ensure that the loading rate used was low enough to eliminate rate effects in the predicted plate stiffness. The force-displacement history was obtained by tracking the total reaction force at the symmetry line. The displacement-time histories of the series of nodes, which correspond to the location of one of the inscribed lines (line 1, 5 mm from the notch mid-plane) were also collected.

RESULTS AND DISCUSSION

Before proceeding with an overview of the results it is helpful to define a few terms. First, the *notch* refers to the pre-formed through-thickness saw cut in the specimen. A *crack* is a zone of damage ahead of the notch which contains a combination of fibre damage, matrix cracking, and delamination which cause a through-thickness discontinuity in the material (i.e. a through

crack, with no load carrying capability across the damaged zone). In contrast, the *process zone*, which leads the crack, contains some matrix and/or fibre damage, and/or delaminations but only in some of the plies (i.e. there is still a continuous load path across the damaged zone).

Force-Displacement Response

An example of the force-displacement response measured experimentally is shown in Fig. 4. The initial elastic response is followed by damage growth (indicated by the saw-tooth response), and ultimately crack growth with the corresponding sudden load drop. The inset figure in the upper right corner of Fig. 4 summarizes the results of the deplies and micrographical analyses and shows the extent of the damage zone which had developed at each of the points labelled on the experimental curve in Fig. 4.

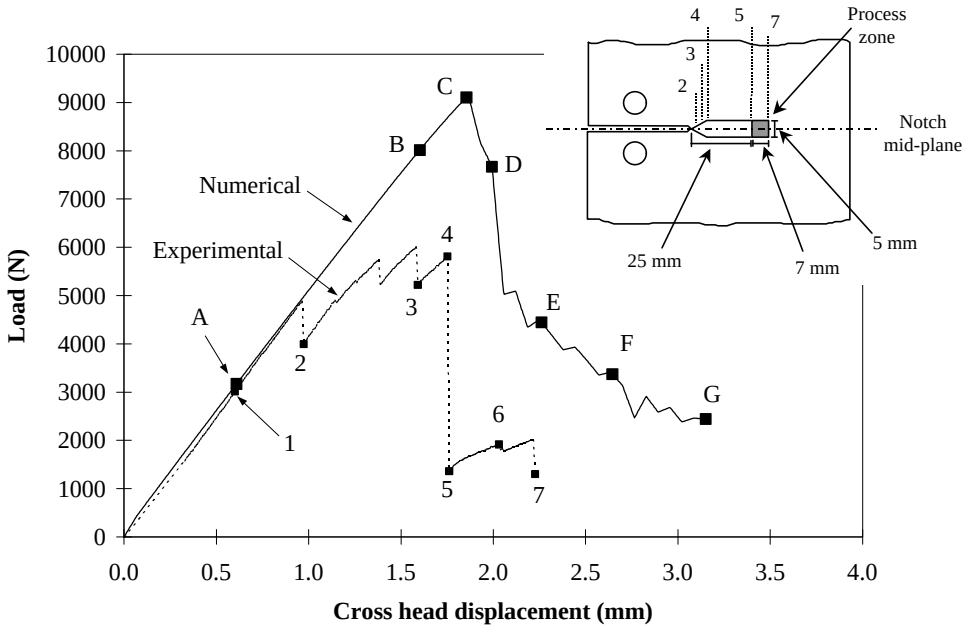

Fig. 4: Experimentally measured and predicted cross-head force-displacement curves and corresponding experimentally measured extent of damage growth. The reference points are used to compare the measured and predicted displacement fields and damage growth in Figs. 7 and 8 below. (Adapted from Ref. 2)

It is interesting to note that up to State 4, damage growth consists of the development of a wider and wider zone of damage but not extension of the notch in the form of a crack. From State 4 to State 5, the micrographical analysis confirms the sudden extension of the crack. This crack growth is stable. That is, the crack is arrested and another process zone develops ahead of the crack (i.e. State 5). This is followed by further extension of the crack (State 7). The width of the damage zone is consistent along the length of the crack and was found to be 5 mm.

Fig. 5 shows the comparison of measured and predicted cross-head force-displacement curves. The three experimental results shown (designated A1, A2, and A3) are repeats of the same geometry and material. Note that the displacements shown in the graph are the total displacements (e.g. the total displacement of one loading pin relative to the other). The predicted peak force and displacement at the onset of crack growth are extremely close to those measured in specimen A1. The change in the slope observed in the predicted force-

displacement curve (i.e. the change in the plate stiffness), is indicative of the initiation of a significant damage growth (i.e. significant stiffness reduction). This damage occurs at roughly the same displacement as the first small load drops (i.e. initiation of significant damage growth) that are observed in the A1 and A2 specimens.

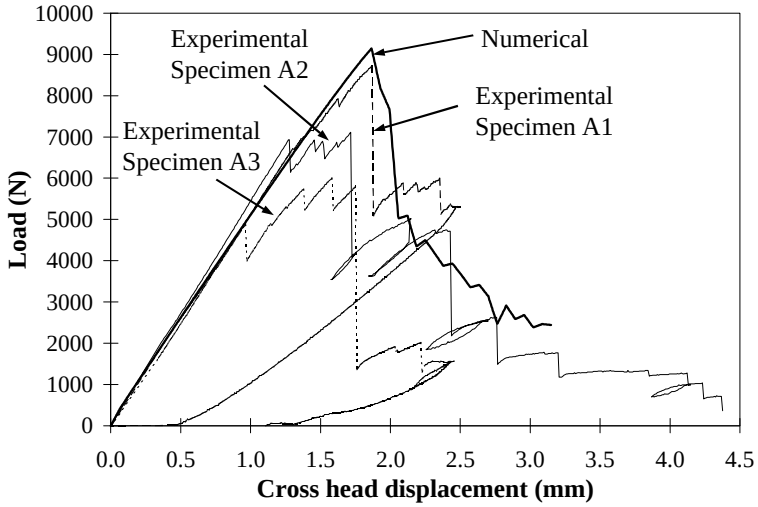

Fig. 5: Comparison of experimentally measured force-displacement curves with the corresponding numerical prediction. Note the range of responses measured from the different experimental specimens, all of which have the same geometry.

It is particularly interesting to note the range of behaviours observed experimentally. The A1 specimen shows a much more brittle response with a higher peak force than either of the other two specimens and a more sudden crack growth (i.e. no significant softening before the load drop). Specimen A3 shows a more gradual development of damage while the response of the A2 specimen falls between that of A1 and A3. These results show that the differences observed between the predicted and measured response in Fig. 4 are within the variability range of the experimental results shown in Fig. 5.

Damage Growth

As mentioned above, a unique feature of these tests is the line analysis used to measure the displacement field on either side of the crack and growing zone of damage. Experimental line analysis results were only available for the A3 specimen. Selected experimental results from the lines inscribed 5 mm from the notch mid-plane are shown in Fig. 6. The experimental and numerical data line analyses correspond to the states labelled **1**, **2**, etc., and **A**, **B**, etc., respectively, in Fig. 4. The difference in the response past the initial load drop complicates the selection of points based solely on cross-head displacement. However, we are more interested in the predictions of displacement field at characteristic points (e.g. just before or just after the load drop). As a result, State A is compared to State 1, B to 3, E to 5, and finally G to 7.

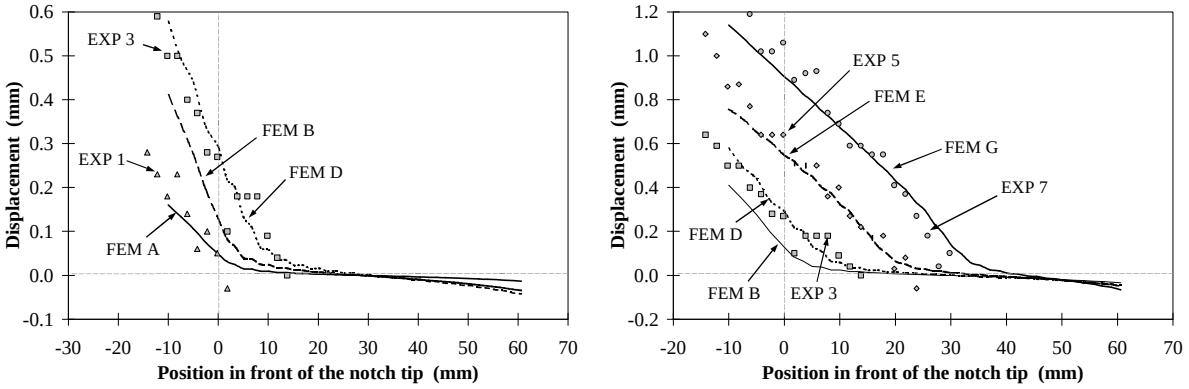

(a) *(b)*

Fig. 6: Comparison of predicted line 4 displacements with experimental measurements. The labels of the experimental and FEM data correspond to the points highlighted on the force-displacement curve shown in Fig. 4.

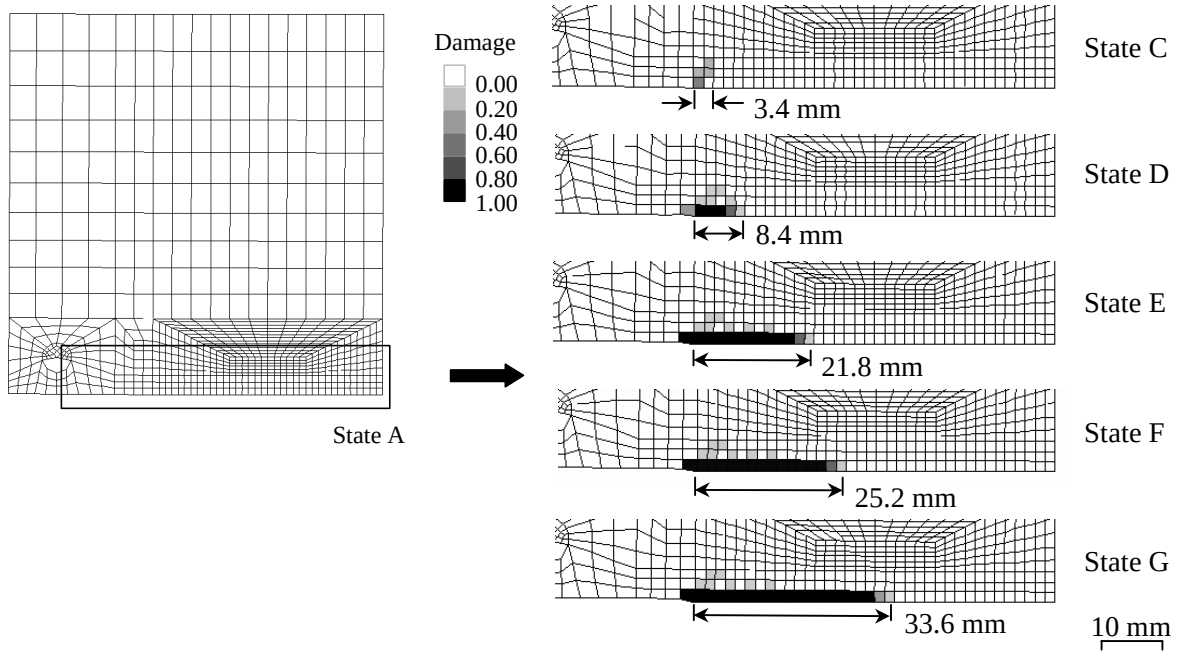

Fig. 7: FEM predictions of damage growth. States correspond to the points highlighted on the force-displacement curve shown in Fig. 4.

Fig. 7 shows the corresponding predictions of damage growth through fringe plots of damage (taken to be an average of damage in two principal directions), again at states corresponding to the labelled points in Fig. 4.

Kongshavn and Poursartip [2] noted that a change in slope of the experimental trend line was indicative of the growth of the process zone. On the other hand, crack growth was accompanied by a shift in the displacement field. Through these results, Kongshavn and Poursartip were able to show that this displacement field analysis can be used as an indication of the development of damage and the extension of the crack. Further, the results indicate that the zero intercept of the experimental trend line gives a quantitative measure of the extent of damage growth (i.e. the location of the leading edge of the process zone). The agreement between the numerical and experimental results in Figs. 6a and b is extremely good. The

overall trends are captured, as are the magnitudes of the displacements indicating that the overall plate stiffness reduction is accurately modelled.

The line analysis in Fig. 6a from the numerical model shows a change in the slope of the displacement field between States A and B but little shift in the zero displacement intercept, an indication of the growth of a damage zone but not crack growth. The linear portion of the predicted trends for A and B, when extrapolated to the axis, shows that the zero displacement occurs at roughly 4 mm, corresponding to a 2 element (3.4 mm) damage zone. This can be compared to the predicted damage zone size at State C, immediately before the predicted load drop, in Fig. 7. The predicted displacement field in Fig. 6a, shows a shift in the curve between States B and D (not a change in slope as was observed between A and B) that can be attributed to crack growth in the experimental results. In Fig. 7 we note the development of a zone of fully damaged elements behind a smaller, partially damaged zone totalling 8.4 mm in length. The numerical line analysis predicts a zero displacement occurring at approximately 10 mm. The same is true from States D to E, and E to G. In all cases, a fairly accurate prediction of the damage growth (Fig. 7) can be made by extrapolating the linear portion of the displacement field back to a zero-displacement, the same technique that was verified experimentally by Kongshavn and Poursartip.

As a final comparison, we return to the experimental damage growth prediction shown in Fig. 4. Experimentally, the process zone size is observed to be approximately 7 mm long. This is roughly the size of the damage zone just before crack growth (labelled as point 4 in Fig. 4). The numerical prediction from States C and D in Fig. 7 show a damage zone that is 3.4 mm before and 8.4 mm after crack growth. The initial state (B) is made up of partially damaged elements only (i.e. a process zone not a crack). After the load drop, the size of the experimental damage zone (crack and process zone) is 25 mm long. The numerical predictions for States E and F are 21.8 and 25.2 mm, respectively. The overall damage zone size (point 7 in Fig. 4) is 32 mm. From State G in Fig. 7 it is predicted to be 33.6 mm. Finally, the width of the experimental damage is 5 mm. While the width of the predicted damage zone varies along its length, the initial process zone at States C and D are predicted to be between two and three elements in width or 3.36 to 5.04 mm. In all cases, the predicted damage zone sizes are remarkably similar to the measured values.

CONCLUSIONS

A new constitutive model, CODAM3Ds, based on CDM has been developed and implemented into LS-DYNA3D. The input parameters required to characterize the model are based on simple physical reasoning and widely available material characterization data. One of the main features of this model, which makes it advantageous over other CDM based models, is that it lends itself to physically meaningful predictions of damage size and distribution that can be compared directly with experimental measurements. Results presented here show the predictive capability of the model in terms of overall damage zone size and material response for a problem involving quasi-static in-plane loading.

ACKNOWLEDGEMENTS

The authors gratefully acknowledge the financial support that has been provided by the Canadian Department of National Defence through various contracts with DREV, as well as The Boeing Company, Seattle, and the Natural Sciences and Engineering Research Council of Canada. We would like to thank many of the present and past members of the Composites Group at UBC who have made significant contributions to the work reported in this paper. In

particular, the experimental work of Ingrid Kongshavn has played a pivotal role in the model development and validation. We would also like to acknowledge many interesting discussions and influences from our colleagues at The Boeing Company.

REFERENCES

1. Ilcewicz, L.B., Walker, T.H., Murphy, D.P., et al., "Tension Fracture of Laminates for Transport Fuselage, Part 4: Damage Tolerance Analysis", *Fourth NASA/DOD Advanced Composite Tech. Conference*, NASA CP-3229, 1993, pp. 265-298.
2. Kongshavn, I. and Poursartip, A., "Experimental Investigation of a Strain Softening Approach to Predicting Failure in Notched Fibre Reinforced Composite Laminates", *Composites Science and Technology*, Vol. 59, No. 1, 1999, pp. 29-40.
3. Krajcinovic, D., "Continuum Damage Mechanics", *Applied Mechanics Review*, Vol. 37, No. 1, 1984, pp. 1-6.
4. Chaboche, J.L., "Continuum Damage Mechanics. I. General Concepts", *Journal of Applied Mechanics*, Vol. 55, No. 1, 1988, pp. 59-64.
5. Williams, K.V., "A Physically-Based Continuum Damage Mechanics Model for Numerical Prediction of Damage Growth", Ph.D. Thesis, Dept. of Metals and Materials Engineering, The University of British Columbia, Vancouver, BC, Canada, 1998.
6. Williams, K.V., Vaziri, R., Floyd, A.M., Poursartip, A., "Simulation of Damage Progression in Laminated Composite Plates Using LS-DYNA", *Fifth International LS-DYNA Conference*, Southfield, Michigan, September 21-22, 1998.
7. Hallquist, J.O., "LS-DYNA Theoretical Manual", Livermore Software Technology Corporation, Livermore, CA, 1998.
8. Dost, E.F., Ilcewicz, L.B., Avery, W.B., and Coxon, B.R., "Effects of Stacking Sequence on Impact Damage Resistance and Residual Strength for Quasi-Isotropic Laminates", *Composite Materials: Fatigue and Fracture (Fifth Volume), ASTM, STP1110*, Martin, R.H., Ed., Philadelphia, PA, 1991, pp. 476-500.
9. Highsmith, A.L. and Reifsnider, K.L., "Stiffness-Reduction Mechanisms in Composite Laminates", *Damage in Composite Materials: Basic Mechanisms, Accumulation, Tolerance, and Characterization, ASTM STP 775*, Reifsnider, K.L., Ed., Philadelphia, PA, 1982, pp. 103-117.
10. Poursartip, A., Ashby, M.F., and Beaumont, P.R., "The Fatigue Damage Mechanics of a Carbon Fibre Composite Laminate. I. Development of the Model", *Composites Science and Technology*, Vol. 25, 1986, pp. 193-218.
11. Razi, H., The Boeing Company, Seattle, WA, March, 1995 (Private communication).
12. Williams, K., Kongshavn, I., Poursartip, A., Vaziri, R., et al., "Optimization of the Strain Softening Curve by a Taguchi Method to Model the Notch Behaviour of a Laminated Material", *Sixth AIAA/NASA/ISSMPO Symposium on Multidisciplinary Analysis and Optimization*, Bellevue, WA, Sept. 4-6, 1996, Vol. 2, pp. 1116-1121.